Earth and Planetary Science Letters 306 (2011) 272–278

Contents lists available at ScienceDirect

Earth and Planetary Science Letters

journal homepage: www.elsevier.com/locate/epsl

Temperature variations of constitutive parameters can significantly affect the fault dynamics

Andrea Bizzarri *

Istituto Nazionale di Geofisica e Vulcanologia, Sezione di Bologna, Via Donato Creti, 12-40128 Bologna, Italy

ARTICLE INFO

Article history:
Received 2 February 2011
Received in revised form 4 April 2011
Accepted 11 April 2011
Available online 2 May 2011

Edited by: L. Stixrude

Keywords:
earthquake source dynamics
rheology of faults
frictional heating
earthquake recurrence
computational seismology

ABSTRACT

A rate- and state-dependent governing law with temperature-dependent constitutive parameters is considered on the basis of laboratory inferences. We model the whole seismic cycle of a homogeneous fault obeying to such a law by adopting a spring-slider dashpot fault analog model. We show that the variations of the parameter a (accounting for the so-called direct effect) with the temperature cause the system to enter, at high speeds, in a conditionally stable regime and also in a velocity strengthening regime. Although we do not observe the complete cessation of slip we can see a severe reduction of the degree of the instability of the fault. In particular, the peaks of the sliding velocity are reduced, as well as the developed temperature due to frictional sliding and the released stress during each instability event. Moreover, the recurrence times are reduced of a factor of two with respect to a reference configuration, where the canonical formulation of rate and state friction (with temporally constant parameters) is assumed. The obtained results can help the interpretation of high velocities laboratory experiments and further illuminate the importance of the temperature in the context of seismic hazard assessment.

1. Introduction

To provide a realistic and consistent description of the dynamics of a seismogenic fault it is mandatory to account for the different physico-chemical processes that can potentially take place during faulting (see Bizzarri, 2009b for a review). As well as spatial heterogeneities of the parameters characterizing the fault and its geometrical irregularities, these dissipative mechanisms can cause dramatic changes in the evolution of the fault traction, and ultimately can have severe implications on the synthetic ground motions, on the simulated stress release and on the recurrence (or inter-event) time of earthquakes occurring on the same seismogenic structure.

Laboratory experiments on simulated faults, geological observations and accurate numerical simulations emphasize the prominent role of the temperature in the earthquake source physics (e.g., Noda et al., 2009).

In the framework of the governing models with cohesion (Ida, 1972; Ruina, 1983) the frictional resistance in a discontinuity interface (the fault surface) evolves through time as a function of the cumulated slip (Andrews, 1976), the average contact time of micro-asperity contacts (Dieterich, 1978) and so on. These dynamic variables are non stationary fields that provide time dependence to the fault traction, which is controlled by some governing parameters. While the spatial heterogeneities of these constitutive parameters have been previously explored (e.g., Bizzarri et al., 2001; Boatwright and Cocco, 1996 among others) in order to simulate the interactions between different fault patches, they have always been kept constant (the only possible exception is represented by Bizzarri, 2010b, who studied the temporal variations of L in next Eq. (3)). The main aim of the present paper is to consider the effects on the dynamics of a planar and spatially homogeneous fault of time-dependent rheological parameters, as inferred from laboratory experiments (Blanpied et al., 1998; Nakatani, 2001).

2. The governing law and the fault model

The fault analog model adopted in this study physically is a harmonic oscillator, in which a block of mass m (per unit surface), sliding on a planar interface and subject to a frictional resistance τ, is loaded by an external applied force (expressed by the temporally constant loading rate $\dot{\tau}_0 = kv_{load}$). The equation of motion we consider is then:

$$m\ddot{u}(t) = k(u_{load} - u(t)) - \tau(t) \tag{1}$$

where the overdots indicate the time derivatives, k is the elastic constant of the spring (that we can associate to the elastic behavior of the medium surrounding the fault), u_{load} is the displacement of the loading point (which slides at the imposed velocity $v_{load} \equiv \dot{u}_{load}$) and u is the displacement (i.e., the fault slip). As emphasized by the standard abuse of notation above, there are no spatial dependencies in the

* Tel.: +39 051 4151432; fax: +39 051 4151499.
E-mail address: bizzarri@bo.ingv.it.

0012-821X/$ – see front matter © 2011 Elsevier B.V. All rights reserved.
doi:10.1016/j.epsl.2011.04.009

variables appearing in Eq. (1); this 1-D fault model can describe the behavior of a generic fault point. The left-hand side term in Eq. (1) represents the inertia, which is accounted for only when the sliding velocity $v \equiv \dot{u}$ exceeds a critical value v_c; below v_c the quasi-static problem is solved (see Bizzarri and Belardinelli, 2008), while above v_c we consider the complete system. Readers can refer to Fig. S1 of the auxiliary material of Bizzarri (2010b) for a schematic representation of the model just described.

Among the large number of constitutive models introduced in the literature to describe the fault dynamics (see Bizzarri and Cocco, 2006b for a discussion), we adopt here the widely-used rate- and state-dependent friction law with true ageing, essentially due to Dieterich (1978), which reads (see also Scholz, 1998):

$$\begin{cases} \tau = \left[\mu_* + a(t)\, ln\left(\frac{v}{v_*}\right) + b(t)\, ln\left(\frac{\Psi v_*}{L}\right)\right]\sigma_n^{eff} \\ \frac{d}{dt}\Psi = 1 - \frac{\Psi v}{L} \end{cases} \tag{2}$$

where a, b, and L (sometimes indicated with symbols D_c or d) are the parameters accounting for the so-called direct effect of friction, its evolution, and the spatial relaxation of the state variable Ψ, respectively. Physically, a and b account for the effects of thermally-activated exponential creep occurring at the microscopic level and govern the macroscopic processes of earthquakes, as well as the formation of faults by strain rate localization. In Eq. (2) μ_* and v_* are reference (constant) values for the frictional coefficient and sliding velocity, respectively and σ_n^{eff} is the effective normal stress, that is assumed to be constant in the present study, since we disregard its variations due to thermal pressurization of pore fluids, considered elsewhere (Bizzarri, 2011; Bizzarri and Cocco, 2006a).

In this empirical constitutive model – which provides a phenomenological description of friction evolution observed in laboratory experiments – we have explicitly stated that parameters a and b might vary through time. In particular, in this study we will consider the following relation, expressing a linear dependence of a on the temperature T due to frictional heating:

$$a = \frac{k_B}{V_a h} T \tag{3}$$

as inferred in laboratory experiments by Blanpied et al. (1998) and Nakatani (2001). In Eq. (3) k_B is the Boltzmann's constant ($k_B = 1.38 \times 10^{-23}$ J/K), V_a is the activation volume ($V_a = q\Omega\, k_B/R$, where q is a dimensionless constant, Ω is the effective molecular volume and R is the gas constant; Gordon, 1967; Sleep, 1997), h is the hardness (within the framework of the classical adhesion theory, we have: $h = A_m \sigma_n / A_{ac}$, where A_m and A_{ac} are the nominal and real contact areas, respectively, and σ_n is the macroscopic normal stress; Holm, 1946) and T is the absolute temperature. In this study we will consider that T is not an experimental, externally-imposed condition, but that it is due to the frictional heating. In this case T is expressed analytically as (Bizzarri and Cocco, 2006a):

$$T(t) = T_0 + \frac{1}{2cw}\int_0^t dt'\; erf\left(\frac{w}{2\sqrt{\chi(t-t')}}\right)\tau(t')v(t') \tag{4}$$

where c is the heat capacity for unit volume, χ is the thermal diffusivity, erf(.) is the error function and w is the half-thickness of the slipping zone where the slip is concentrated in a "Chester-type" fault (Bizzarri, 2009b and references cited therein). The dependence of a on T can result faster than linear if we consider an additional dependence of h on the temperature, accounting for plastic deformation of asperity contacts (Noda, 2008). Here we consider that h is a bulk material constant, that is the explicit dependence on T in Eq. (3) dominates. Incidentally, we mention that also V_a can be temperature-dependent (or even pore fluid-dependent). When coupled with Eq. (3) Eq. (4) gives an implicit temporal dependence to the parameter a.

In the remainder of the paper we will consider two different configurations, Model A and Model B, that are the two end members

Table 1
Reference parameters of the present paper. Initial conditions refer to $t = 0$.

Parameter	Value	
Model parameters		
Tectonic loading rate, $\dot{\tau}_0 = k v_{load}$	3.17×10^{-3} Pa/s (= 1 bar/yr)	
Machine stiffness, k	10 MPa/m[a]	
Period of the analog freely slipping system, $T_{a.f.} = 2\pi\sqrt{m/k}$	5 s	
Critical value of the sliding velocity above which the dynamic regime is considered, v_c	0.1 mm/s	
	Model A	Model B
Fault constitutive parameters		
Effective normal stress, σ_n^{eff}	30 MPa	
Initial value of the logarithmic direct effect parameter, a_0	9.3394×10^{-3}	1.2708×10^{-2}
Increasing rate of the parameter a	2.5029×10^{-5} K^{-1}	3.4055×10^{-5} K^{-1}
Initial value of the evolution effect parameter, b_0	0.016	
Resulting $b_0 - a_0$ difference	6.6606×10^{-3}	3.2923×10^{-3}
Characteristic scale length for the state variable evolution, L	7 mm	
Reference value of the friction coefficient, μ_*	0.56	
Reference value of the sliding velocity, v_*	3.17×10^{-10} m/s (= 1 cm/yr)	
Initial slip velocity, v_0	3.17×10^{-10} m/s	
Initial value of state variable, Ψ_0	$\Psi^{ss}(v_0) = L/v_0 = 22.08 \times 10^6$ s[b]	
Initial shear stress, τ_0	$\tau^{ss}(v_0) = \mu_* \sigma_n^{eff} = 16.8$ MPa[b]	
Initial temperature, T_0	373.15 K (= 100 °C)	
Heat capacity for unit volume of the bulk composite, c	3×10^6 J/(m^3 K)	
Thermal diffusivity, χ	1×10^{-6} m^2/s	
Slipping zone thickness, $2w$	1.5 mm	
Activation volume, V_a	$(0.41\text{ nm})^3$	$(0.37\text{ nm})^3$
Hardness, h	8 GPa[c]	

[a] With the initial values of the constitutive parameters this corresponds to an unstable regime, in that $k < k_{cr_0} \equiv (b_0 - a_0)\sigma_n^{eff}/L = 28.55$ MPa/m and 14.11 MPa/m for Models A and B, respectively (Gu et al., 1984). The resulting k_{cr0}/k ratios are 2.86 and 1.41, respectively.
[b] The system starts at $t = 0$ from its steady state (at a generic time t_* the steady state is defined by the condition $\frac{d}{dt}\Psi|_{t=t_*} = 0$).
[c] See Bowden and Tabor (1964).

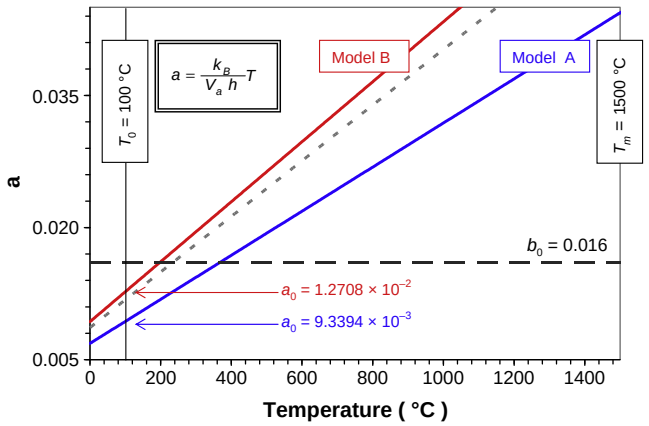

Fig. 1. Representative evolution of the parameter a with the temperature, as given by Eq. (3). The dotted line represents a linear extrapolation of data from Ruina (1983). Dashed line indicates the reference value of b. Parameters are listed in Table 1.

reported by Nakatani (2001) and that characterize two different instability regimes of a fault (Model A is unstable, while Model B is moderately unstable).

3. A numerical example

As a first case study, in this section we conservatively assume that the parameter b in the constitutive model (2) varies through time, such that the difference $b(t)-a(t)$ equals b_0-a_0 at all times. The parameter a evolves accordingly to Eq. (3). There are no experimental measures demonstrating that b directly depends on the temperature in the same way as a does, but we simply want to analyze the effects of the temporal variations of a in the simplest case. We recall here that there are evidences suggesting that also a–b depends on T (e.g., Blanpied et al., 1998; He et al., 2007). Incidentally, we mention that Sleep (2006) has shown that a–b can depend on the slipping zone thickness $2w$, which is constant in the present study, but in general can vary (Bizzarri, 2010b). We will examine in the next section the case of varying a and constant b. The adopted parameters are reported in Table 1, Model A.

Fig. 2 reports the results of the comparison between a reference case, with both constants a and b (black curves) and the test case described above, where both a and b change through time (red curves). We can clearly see from Fig. 2a and b that the response of the system is quite similar in the two simulations, in that the time occurrence of the repeated instabilities is the same (we recall here that an instability is defined when v exceeds a limiting velocity, v_l; see Bizzarri and Belardinelli, 2008 and references therein). Moreover, we observe that the peaks in v are comparable (Fig. 2a), as well as the traction evolution and thus the temperature change (Fig. 2b), as resulting from Eq. (4).

There are two nondimensional parameters characterizing the degree of instability of a fault governed by rate and state friction (e.g., Gu et al., 1984; Ruina, 1983):

$$\kappa = \frac{k_{cr}}{k} = \frac{B-A}{kL} \tag{5}$$

and

$$\beta = \frac{B}{A} \tag{6}$$

in which $A \equiv a\sigma_n^{eff}$ and $B \equiv b\sigma_n^{eff}$. The more κ and β exceed 1 the more unstable the fault is, i.e., peaks in v and the stress releases are larger. In all the present simulations the effective normal stress is temporally constant and both a and b vary concurrently (see Fig. 2c), such that κ is constant through time and β is always greater than the unity. This explains why the response of the system is very similar in the two numerical experiments. When σ_n^{eff} is constant through time β equals b/a and it has been interpreted as the relative efficiency of the grain lattice in aiding frictional sliding versus compaction (Sleep, 1997).

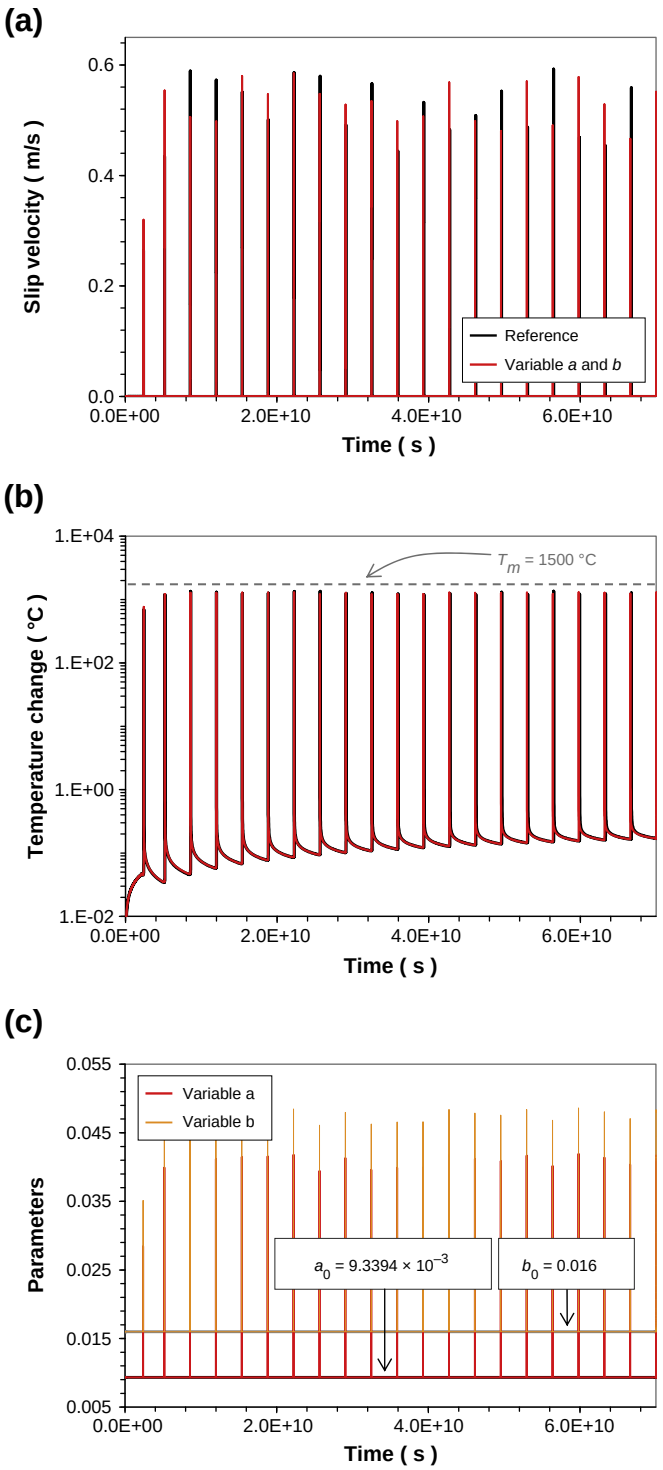

Fig. 2. Comparison between a reference model, having both a and b constant (black lines), and a test case where a varies accordingly to Eq. (3) and b changes such that $b(t)-a(t)=b_0-a_0$ for all times (red lines). Time evolutions of the slip velocity (panel (a)), of temperature change (T–T_0; panel (b)) and of constitutive parameters a and b (panel (d)). In panel (b) T_m emphasizes that melting regime is not reached by the system. Parameters refer to Model A of Table 1.

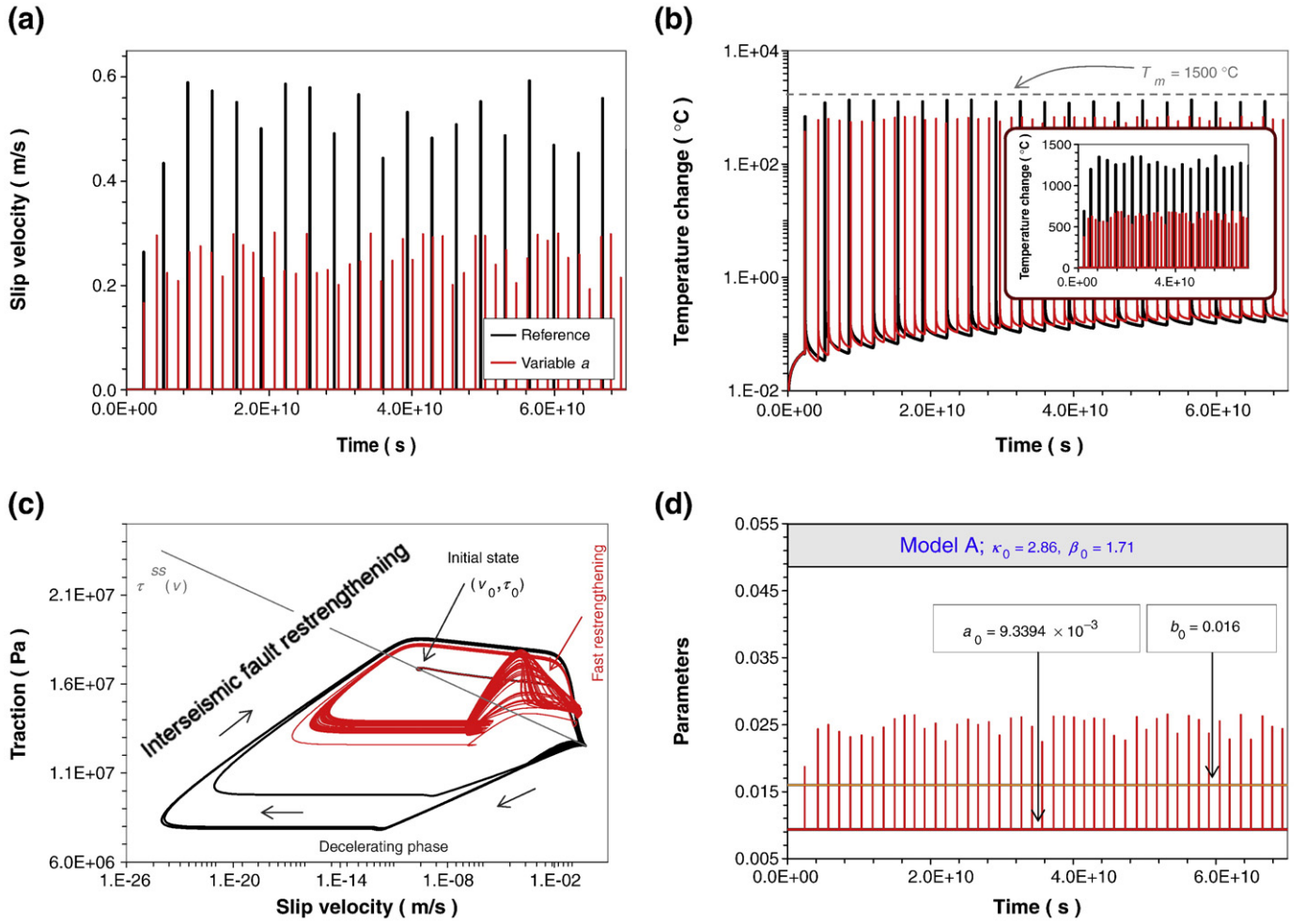

Fig. 3. Comparison between the reference model (black curves), and Model A where only parameter a is varying (red curves). (a) Time histories of slip velocity; note the reduction of peaks in slip velocity roughly from 0.6 m/s to 0.3 m/s. (b) Time histories of temperature change (with inset in linear scale). (c) Phase portrait (i.e., traction vs. slip velocity). The steady state traction for the reference configuration, defined as $\tau^{ss}(v) = \mu_* \sigma_n^{eff} + (B-A)\ln\left(\frac{V_*}{v}\right)$, is reported in gray. (d) Time evolution of the constitutive parameters a and b. Values of parameters κ and β (Eqs. (5) and (6), respectively), at $t=0$, are also given.

All the previous results hold also for Model B (the plots are not shown for brevity).

4. Influence of a temperature-dependent rheology on earthquake instabilities

The conditions guaranteeing an unstable behavior ($\kappa>1$ and $\beta>1$) are not necessarily satisfied when b is kept constant ($b(t)=b_0, \forall\, t\geq 0$) and only a varies though time. This is the case we consider in the present section. In Fig. 3 we superimpose the curves pertaining to the reference case (black lines; the same reported in black in Fig. 2) and a case with time-variable a (red lines). Both simulations start from the same initial conditions (Fig. 3c), defining a velocity weakening regime ($\beta>1$), but as long as the system evolves the two cases diverge. In fact, we can now observe that the peaks in v are significantly reduced, roughly of a factor of 2 (Fig. 3a). The same holds for the temperature change (Fig. 3b), in agreement with the theoretical prediction of Eq. (4). Interestingly, the cycle time (i.e., the time interval separating two subsequent instabilities) is significantly reduced (Fig. 3a; see also next Fig. 6).

Moreover, from Fig. 3d we can observe that in the correspondence of the dynamic instability, when the temperature changes are more significant, the parameter a exceeds b, so that $\beta<1$ (see Eq. (6)), a situation defined as velocity strengthening (e.g., Boatwright and Cocco, 1996).

This is clearly visible in Fig. 4, where we report a zoom on a single instability of the case of the time-variable a. When T increases, a correspondently increases by construction (Eq. (3)); at the same time κ approaches 1 and continues to decrease even below 1, defining the conditionally stable regime (Gu et al., 1984). At this stage the fault is decelerating, but because the system is already undergoing to an instability, even if $0<\kappa<1$, it does not stop and the fault already experiences a dynamic instability (Fig. 4a). The system has already entered a velocity strengthening regime (emphasized by red portions of the curves in Fig. 4), in that $B<A$ (or equivalently $\beta<1$). This further contributes to decelerate the fault and ultimately leads to a fast restrengthening phase, during which the frictional resistance tends to increase rapidly after the dynamic instability. This phenomenon is clearly visible in Fig. 3c. Interestingly, we remark here that the temperature dependence of the frictional resistance proposed by Chester and Higgs (1992) – which is different with respect to that of Eq. (3) – also causes a fast restrengthening mechanism and this increase in frictional resistance can be sufficiently pronounced to cause the rupture to stop and the so-called self-healing rupture mode of propagation (Bizzarri, 2010a).

It is also interesting to explore how the system behaves in the case of the evolution of a as in Model B (red line in Fig. 1). The correspondent

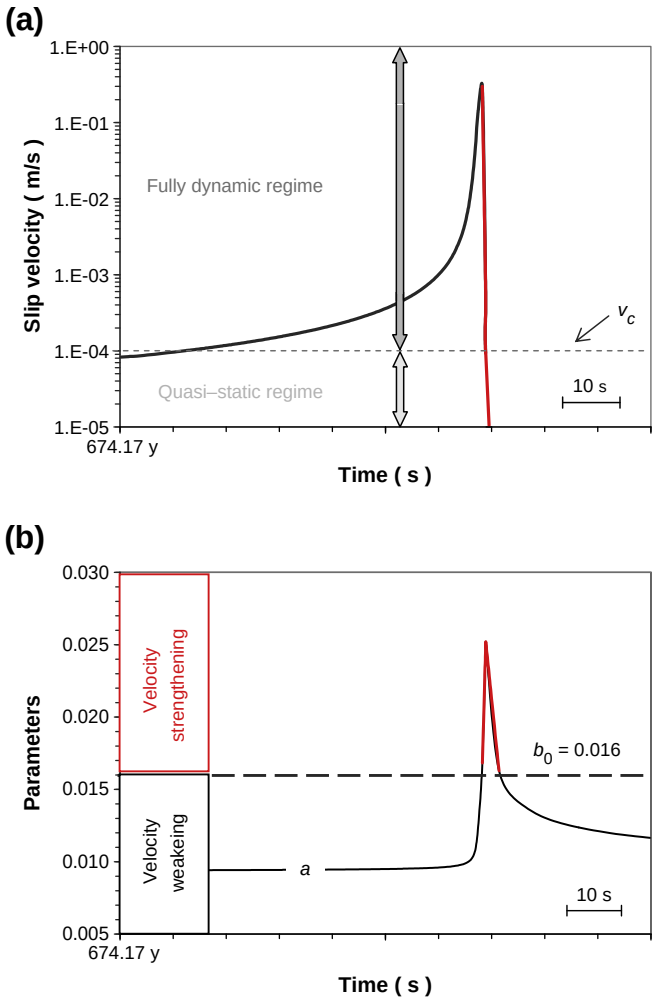

Fig. 4. Zoom of the evolution of the slip velocity (in logarithmic scale; panel (a)) and of governing parameters (panel (b)) in the case of time-variable a (reported in the whole time window in Fig. 3 with red lines). Red portions of the curves denote the velocity strengthening regime (in which $b(t)<a(t)$).

results are plotted in Fig. 5, where again we superimpose the reference case, where a and b are kept constant over the whole time window. In this case the fault is moderately unstable (now, at $t=0$, we have: $\kappa_0=1.41$ and $\beta_0=1.26$ instead of $\kappa_0=2.86$ and $\beta_0=1.71$ as in Model A); the reference case, compared to the reference case of Model A, exhibits a longer interval before the first instability, lower peaks in v (Fig. 5a) and smaller temperature changes (Fig. 5b). The latter ultimately cause smaller variations in the parameter a (compare Figs. 5d and 3d). Nevertheless, also in the present Model B during the instabilities the conditionally stable regime ($\kappa<1$) and the velocity strengthening regime ($\beta<1$) are reached by the system when a is varying. Also in this numerical simulation the slider accelerates to instability, but the effects of the variations of a are even more relevant: now peaks in v are reduced by nearly a factor of 10 with respect to the reference case (Fig. 5a) and the temperature change is reduced roughly by a factor 3 (Fig. 5b). As for Model A, we still highlight a reduction of the seismic cycle; this is due to the fact that in the case of time-variable a the stress release is smaller (with respect to the reference case; see Fig. 5c) due to increased strengthening and the minimum of v after instability is greater. Therefore the stress increase required after a dynamic event to reach again the failure point (the peak of traction) is smaller than in the case of constant a.

A synoptic comparison between the cycle times obtained in the numerical experiments discussed above is reported in Fig. 6. For both Models A and B we can observe that the temporal variations of parameter a cause the reduction of the seismic cycle roughly by a factor of 2 with respect to the reference configurations, having a constant a (the cycle time decreases from 108 y to 50 y for Model A and from 51 y to 25 y for Model B). This indicates that, together with the thermal pressurization of pore fluids (Mitsui and Hirahara, 2009) and the wear processes (Bizzarri, 2010b), also the inclusion of the temperature-dependence on the direct effect of the rate and state friction can significantly modify the seismic cycle.

5. Conclusions and outlook

Indubitably, the most severe effect of the temperature on the rheology of fault zones is represented by the melting of rocks and gouge materials. In such a case the Coulomb framework is no longer valid, since the rocks behave essentially as viscous fluids and a different rheology has to be assumed to model the fault dynamics after the melting point (Bizzarri, 2011). In the present paper we exclude the bulk melting by assuming parameters that led to temperatures that remain below the (average) melting temperature (see Figs. 2b, 3b and 5b). Moreover, laboratory experiments indicate that numerous thermally-activated processes can take place at high speeds, such as mechanical lubrication, thermal pressurization, flash heating (see Bizzarri, 2009b for a comprehensive review).

On the other hand, performing low-velocity laboratory experiments Chester and Higgs (1992) and Chester (1994) found direct evidences of a dependence of the temperature (T) on the response of the synthetic fault and they interpreted the data by proposing a rate-, state- and temperature-dependent friction law, which generalizes the "classical", or canonical formulation (e.g., Ruina, 1983). Spontaneous dynamic model of 3-D faults indicates that such a governing model can provide a suitable mechanism to reproduce the self-healing mode of propagation, in which the fault slip heals after some time (in other words the fault slip velocity has a compact support; Bizzarri, 2010a).

In the present work we consider an alternative interpretation of a temperature-dependent rheology, as suggested by low-velocity laboratory experiments of Blanpied et al. (1998) and Nakatani (2001), who postulate that the parameter a in the classical analytical expression of the rate and state friction linearly varies with T (see Eq. (3); see also Heslot et al., 1994; Sleep, 1997). Physically, this accounts for the thermally-activated, Arrhenius-like creep processes occurring at the asperity contacts level, where the real stresses are GPa in magnitude (Bréchet and Estrin, 1994; Nakatani and Scholz, 2004). The parameter a modulates the slip-hardening stage of a fault preceding an earthquake failure, and, since T evolves through time as a function of the heat input ($\tau v/2w$; see Eq. (4)), a also varies through time, depending on the rupture history.

To date, this is the first example of the simulation of the whole seismic cycle accounting for time-variable rheological parameters. Indeed, our numerical simulations with a spring-slider system demonstrate that such temporal variations of a can have relevant effects on the evolution of the fault during its life, in that they will delocalize strain in a finite width slip zone (a similar result was obtained by Sleep, 1997, who increased the parameters μ_* of Eq. (2) with the temperature, as done in Bizzarri, 2010a).

We have shown that the system can spontaneously reach the conditionally stable regime ($\kappa<1$; see Eq. (5)) and even the velocity strengthening regime ($\beta<1$; see Eq. (6)). The velocity strengthening regime has received much attention because it appears to be able to explain the inferred decrease in cosesimic slip toward the Earth's surface (Fialko et al., 2005). The fault experiences a fast restrengthening (clearly visible in Fig. 3c), which is not sufficient to prevent the instability from occurring or to stop the rupture (as could happen

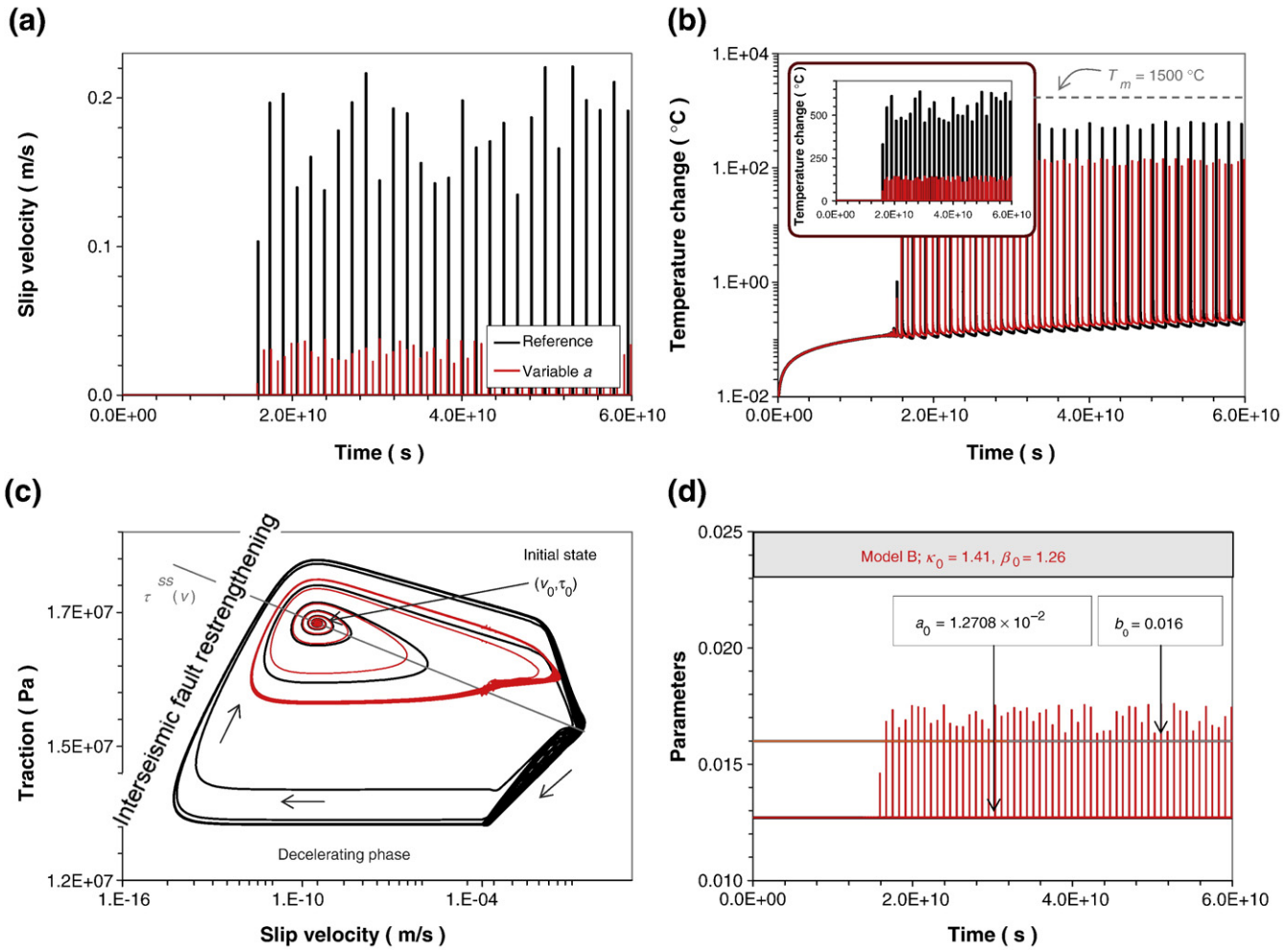

Fig. 5. The same as Fig. 3, but now for Model B. Note the change in the values of the ordinates. In this case we have a reduction of peaks in slip velocity roughly from 0.2 m/s to 0.02 m/s.

when the flash heating of micro-asperity contacts is considered; Bizzarri, 2009a; Noda et al., 2009).

The variations of a also cause a significant reduction of the peaks in fault slip velocity (roughly of a factor of 2 for Model A and of a factor of 10 for Model B; Figs. 3a and 5a, respectively) and a reduction of temperature change due to the frictional heating (approximately of a factor of 2 for Model A and of a factor of 3 for Model B; Figs. 3b and 5b, respectively). The reduction of the peaks in v can solve the physical paradox of extremely large slip velocities, often resulting from numerical experiments (Noda et al., 2009). This reduction has its counterpart in the diminution of the developed slip, suggesting (in a more complex 3-D fault model) a decrease of the size (i.e., the seismic moment) of the earthquake events.

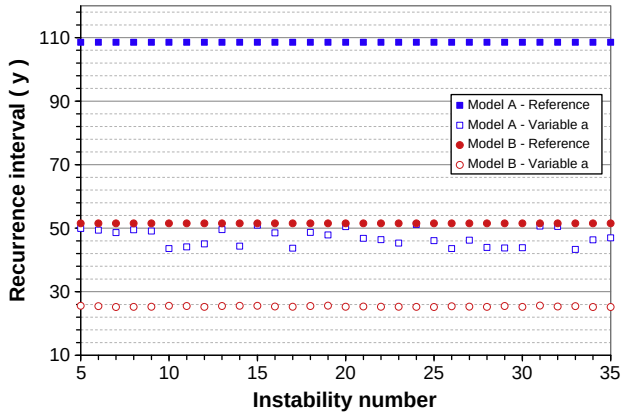

Fig. 6. Behavior of the cycle time for the two models (Model A is in black; Model B is in gray). Full symbols refer to the reference configurations, with constant governing parameters, while empty symbols refer to cases with variable *cix*. The instabilities are plotted starting from the fifth event to avoid possible effects of the initial conditions (transient stage).

Moreover, we have found here that the stress released after each instability is reduced with respect to the reference configurations (Figs. 3c and 5c), while the minima of the slip velocity after the dynamic event are larger. This implies that interseismic fault restrengthening is faster in cases with variable a and therefore the seismic cycle is shorter in these cases, as confirmed by Fig. 6. The significant reduction of the recurrence time (roughly of a factor of 2 in our numerical experiments) demonstrates that a temperature-dependent rheology adds further complication in the attempt to estimate the seismic cycle, even for an isolated fault with spatially homogeneous properties.

The effects discussed above are similar to those obtained when wear mechanisms are considered in a fluid-saturated fault (Bizzarri, 2010b). However, we emphasize that in that situation the fault does not enter the velocity strengthening regime, since the parameter β remains constant through time (the variations of A and B due to time changes in σ_n^{eff} are the same), contrarily to the present case of time-variable a, in which β oscillates above and below the unity.

It is interesting to mention that time-dependent restrengthening of fault zones through solution-aided mechanisms can result in significantly

stronger fault zones (e.g., Nakatani and Scholz, 2004, Niemeijer et al., 2008, Tenthorey and Cox, 2006). Presumably, the value of $b–a$ changes during this phase along with the friction. In fact, there are some indications that a increases significantly during hold periods as a result of densification of the gouge, which would be interesting to include in future studies.

We emphasize that the most important changes in the frictional resistance occur at high speeds (Fig. 4a), when temperature changes are also more relevant; here the system is in the velocity strengthening regime. Indeed, Shimamoto (1986) and Shimamoto and Hirose (2005) report for halite and gabbro a velocity strengthening behavior at high speeds, acting as a barrier in earthquake nucleation processes. We recall here that in the present study we neglect other thermally-generated mechanisms, such as flash weakening, bulk melting, thermal pressurization of pore fluids and powder lubrication, that might cause a further significant weakening.

Given the intrinsic limitations of the spring-slider analog fault model our results indicate that the temperature-dependence in the direct effect of friction can be envisaged as a good candidate to interpret the laboratory data at high speeds realized with the new-generation laboratory machines and further confirm the importance of the temperature in the context of the seismic hazard assessment.

Acknowledgements

I wish to place on record my indebtedness to A. Niemeijer, to N. Sleep and to the Editor L. P. Stixrude for their constructive and stimulating comments that contributed to improve the manuscript.

References

Andrews, D.J., 1976. Rupture velocity of plane strain shear cracks. J. Geophys. Res. 81 (No. 32), 5679–5687.
Bizzarri, A., 2009a. Can flash heating of asperity contacts prevent melting? Geophys. Res. Lett. 36, L11304. doi:10.1029/2009GL037335.
Bizzarri, A., 2009b. What does control earthquake ruptures and dynamic faulting? A review of different competing mechanisms. Pure Appl. Geophys. 166 (Nos. 5–7), 741–776. doi:10.1007/s00024–009–0494–1.
Bizzarri, A., 2010a. Pulse-like dynamic earthquake rupture propagation under rate-, state- and temperature-dependent friction. Geophys. Res. Lett. 37, L18307. doi:10.1029/2010GL044541.
Bizzarri, A., 2010b. On the recurrence of earthquakes: role of wear in brittle faulting. Geophys. Res. Lett. 37, L20315. doi:10.1029/2010GL045480.
Bizzarri, A., 2011. Dynamic seismic ruptures on melting fault zones. J. Geophys. Res. 116, B02310. doi:10.1029/2010JB007724.
Bizzarri, A., Belardinelli, M.E., 2008. Modelling instantaneous dynamic triggering in a 3-D fault system: application to the 2000 June South Iceland seismic sequence. Geophys. J. Int. 173, 906–921. doi:10.1111/j.1365-246X.2008.03765.x.
Bizzarri, A., Cocco, M., 2006a. A thermal pressurization model for the spontaneous dynamic rupture propagation on a three-dimensional fault: 1. Methodological approach. J. Geophys. Res. 111, B05303. doi:10.1029/2005JB003862.
Bizzarri, A., Cocco, M., 2006b. Comment on "Earthquake cycles and physical modeling of the process leading up to a large earthquake". Earth Planets Space 58, 1525–1528.
Bizzarri, A., Cocco, M., Andrews, D.J., Boschi, E., 2001. Solving the dynamic rupture problem with different numerical approaches and constitutive laws. Geophys. J. Int. 144, 656–678.
Blanpied, M.L., Marone, C.J., Lockner, D.A., Byerlee, J.D., King, D.P., 1998. Quantitative measure of the variation in fault rheology due to fluid–rock interactions. J. Geophys. Res. 103, 9691–9712.
Boatwright, J., Cocco, M., 1996. Frictional constraints on crustal faulting. J. Geophys. Res. 101 (B6), 13895–13909. doi:10.1029/96JB00405.
Bowden, F.P., Tabor, D., 1964. The Friction and Lubrication of Solids, Part 2. (544 pp.) Oxford Univ. Press, New York.
Bréchet, Y., Estrin, Y., 1994. The e1ect of strain rate sensitivity on dynamic friction of metals. Scripta Met. Mater. 30, 1449–1454.
Chester, F.M., 1994. Effects of temperature on friction: constitutive equations and experiments with quartz gouge. J. Geophys. Res. 99 (No. B4), 7247–7261.
Chester, F.M., Higgs, N.G., 1992. Multimechanism friction constitutive model for ultrafine gouge at hypocentral conditions. J. Geophys. Res. 97 (B2), 1859–1870.
Dieterich, J.H., 1978. Time-dependent friction and the mechanics of stick slip. Pure Appl. Geophys. 116, 790–806.
Fialko, Y., Sandwel, D., Simons, M., Rosen, P., 2005. Three-dimensional deformation caused by the Bam, Iran, earthquake and the origin of the shallow slip deficit. Nature 435, 295–299.
Gordon, R.B., 1967. Thermally activated processes in the Earth: creep and seismic attenuation. Geophys. J. R. astr. Soc. 14, 33–43.
Gu, J.C., Rice, J.R., Ruina, A.L., Tse, S.T., 1984. Slip motion and stability of a single degree of freedom elastic system with rate and state dependent friction. J. Mech. Phys. Solids 32, 167–196.
He, C., Wang, Z., Yao, W., 2007. Frictional sliding of gabbro gouge under hydrothermal conditions. Tectonophys. 445, 353–362. doi:10.1016/j.tecto.2007.09.008.
Heslot, F., Baumberger, T., Perrin, T.B., Caroli, B., Caroli, C., 1994. Creep, stick-slip, and dry-friction dynamics: experiments and a heuristic model. Phys. Rev. E 49, 4973–4988.
Holm, R., 1946. Electric Contacts. (398 pp.) H. Gebers Förlag, Stockholm.
Ida, Y., 1972. Cohesive force across the tip of a longitudinal-shear crack and Griffith's specific surface energy. J. Geophys. Res. 77 (No. 20), 3796–3805.
Mitsui, Y., Hirahara, K., 2009. Coseismic thermal pressurization can notably prolong earthquake recurrence intervals on weak rate and state friction faults: numerical experiments using different constitutive equations. J. Geophys. Res. 114, B09304. doi:10.1029/2008JB006220.
Nakatani, M., 2001. Conceptual and physical clarification of rate and state friction: frictional sliding as a thermally activated rheology. J. Geophys. Res. 106, 13347–13380. doi:10.1029/2000JB900453.
Nakatani, M., Scholz, C.H., 2004. Frictional healing of quartz gouge under hydrothermal conditions: 2. Quantitative interpretation with a physical model. J. Geophys. Res. 109, B07202. doi:10.1029/2003JB002938.
Niemeijer, A., Marone, C., Elsworth, D., 2008. Healing of simulated fault gouges aided by pressure solution: results from rock analogue experiments. J. Geophys. Res. 113, B04204. doi:10.1029/2007JB005376.
Noda, H., 2008. Frictional constitutive law at intermediate slip rates accounting for flash heating and thermally activated slip process. J. Geophys. Res. 113, B09302. doi:10.1029/2007JB005406.
Noda, H., Dunham, E.M., Rice, J.R., 2009. Earthquake ruptures with thermal weakening and the operation of major faults at low overall stress levels. J. Geophys. Res. 114, B07302. doi:10.1029/2008JB006143.
Ruina, A.L., 1983. Slip instability and state variable friction laws. J. Geophys. Res. 88, 10359–10370.
Scholz, C.J., 1998. Earthquakes and friction laws. Nature 391, 37–42.
Shimamoto, T., 1986. Transition between frictional slip and ductile flow for halite shear zones at room temperature. Science 231, 711–714. doi:10.1126/science.231.4739.711.
Shimamoto, T., Hirose, T., 2005. Intermediate-velocity friction barrier and its implication for earthquake generation. EOS Trans. AGU 86, 52 (Fall Meet. Suppl. Abstract T13E–08).
Sleep, N.H., 1997. Application of a unified rate and state friction theory to the mechanics of fault zones with strain localization. J. Geophys. Res. 102, 2875–2895.
Sleep, N.H., 2006. Real contacts and evolution laws for rate and state friction. Geochem. Geophys. Geosyst. 7, Q08012. doi:10.1029/2005GC001187.
Tenthorey, E., Cox, S.F., 2006. Cohesive strengthening of fault zones during the interseismic period: an experimental study. J. Geophys. Res. 111, B09202. doi:10.1029/2005JB004122.